Indian J. Applied & Pure Bio. Vol. 41(1), 441-450 (2026). **ISSN: 0970-2091**

Bioinspired Synthesis of Zinc Oxide Nanoparticles from *Citrus* fruit peel extract, their characterization and agricultural application as plant Growth promoter

Rudiksha Koche[1]*, Ruchita Gandhi[1] and Rupali Shirsat[2]

[1]Department of Botany, Shri Shivaji College of Arts, Commerce, and Science, Akola (MS) 444003 (India)
[2]Department of Botany, Shri Dr. R. G. Rathod Arts and Science College, Murtizapur, District- Akola (MS) 444107 (India)
(Email: kocherudiksha@gmail.com)

Abstract

Over the past few years, agricultural science has ventured into various novel products and technologies, with metal nanoparticles emerging as highly promising tools. They are anticipated to play an important role in modern agricultural practices. As a result, there is an urgent demand for an eco-friendly, safe, and non-toxic approach to tackle the challenges faced in agriculture and the food industry. Furthermore, waste management presents a challenge in both the agricultural and food industries. Citrus sinensis peels, being among the most underutilized and widely available bio-waste residues, present a significant challenge in waste management for the food industry. The present study addresses this issue by demonstrating the synthesis of zinc oxide nanoparticles (ZnO NPs) using extract derived from Citrus sinensis fruit peels. The peel extract serves both as a reducing agent and a precursor for nanoparticle synthesis. Verification of ZnO NPs synthesis was achieved through UV-visible spectroscopy, indicating a distinct peak in between 300-400 nm. Additionally, comprehensive characterization of these bioinspired green-synthesized nanoparticles was conducted using scanning electron microscopy and X-ray diffraction. Scanning Electron Microscopy (SEM) facilitated the examination of particle morphology and size distribution, revealing irregularly shaped crystals predominating among the synthesized nanoparticles. The presence of ZnO NPs was further confirmed through X-ray diffraction analysis detecting the average NPs size about 48nm. On the basis of their size, the synthesized ZnO NPs could be utilized effectively for their agricultural applications. These NPs were found to enhance the germination and growth of Spinach plant at 200ppm concentration.

Key words : ZnO NPs, *Citrus sinensis* peels, UV-visible spectroscopy, X-ray diffraction, Scanning Electron Microscopy (SEM).

In recent times, there has been significant interest in the biosynthesis of nanoparticles (NPs), also known as herbal or green synthesis of NPs. This attention stems from the biocompatibility, low toxicity, and environmentally friendly characteristics of both the synthesis process and the resulting nanoparticle products. Utilizing biological materials such as bacteria, yeast, moulds, microalgae, and plant extracts for NP synthesis offers several advantages, including reduced energy consumption and the application of moderate technology without the need for toxic chemicals[10,15].

Plants stand out as the prime option for the green synthesis of nanoparticles. Plant extracts contain a variety of compounds, including polysaccharides, proteins, amino acids, organic acids, and phytochemicals such as polyphenols, flavonoids, terpenoids, alkaloids, tannins, and alcoholic substances. These compounds have the potential to both reduce and stabilize nanoparticles[1]. Furthermore, plant extracts serve as natural capping agents, simplifying the nanoparticle stabilization process into a single step. These beneficial attributes of plant extracts lead to decreased reagent consumption and, consequently, lower costs, enabling the advancement of large-scale nanoparticle production through an eco-friendly method.

Zinc oxide nanoparticles (ZnO NPs) have shown significant promise in enhancing the growth and yield of food crops. When applied to peanut seeds at various concentrations, Zinc oxide nanoparticles not only significantly improved seed germination, seedling vigor, and overall plant growth but also highlighted the effectiveness of nanoscale treatment, particularly at a concentration of 1000 ppm. Specifically, the application of Zinc oxide nanoparticles with particle sizes up to 50 nm had a notable positive effect, promoting considerable growth in both peanut stems and roots[21]. The enhancing effect of colloidal solution of nanoparticles on cereals' overall growth and development was reported by Batsmomova *et al*.[4]. In rice, ZnO NPs are reported act as nano-fertilizer promoting the overall growth and crop yield[3,24]. ZnO NPs also used as to counter abiotic stress in tomatoes[7]. Thus, the plant growth-promoting and antioxidative features of ZnO NPs are demonstrated by various workers[2, 21].

Given the potential of zinc oxide nanoparticles to drive innovation in agricultural science and research, the study presented designing an experiment for the green synthesis and characterization of these zinc oxide nanoparticles derived from *Citrus sinensis* fruit peel.

Plant extracts preparation :

The peels of *Citrus sinensis* fruits were obtained from local juice shops. They were cleaned thoroughly with distilled water and sterilized by gently rubbing alcohol on both surfaces. Afterward, the peels were dried and ground into a fine powder. 5 gm of this powder was then mixed with 100ml of distilled water and left to soak overnight. The resulting mixture was filtered using a muslin cloth and then centrifuged at 5000 rpm for 10 minutes. The sediment was discarded, and the supernatant was retained for further experimentation. Finally, the extract was stored in a cool, dry place for future use.

Green synthesis of zinc oxide nanoparticles:

5 gm of zinc nitrate hexahydrate [$Zn(NO_3)_2 \cdot 6H_2O$] was added to 100ml of aqueous peel extract and stirred on a magnetic stirrer for 2 hours while observing the development of a brownish-yellow color. The mixture was then kept on a heating mantle at 70 ± 2°C for 6 hours to form a white paste of zinc oxide nanoparticles (ZnO-NPs), which was subsequently oven-dried and ground into a fine powder. Finally, the powder was calcined at 500°C. The resulting ZnO NP powder was stored in a cool and dry place for future use[8].

Characterization of ZnO NPs:

Characterization using UV-Visible Spectroscopy :

UV-visible spectroscopy served as a valuable method for characterizing the structure of nanoparticles. The optical absorption spectra of metal nanoparticles predominantly exhibit surface plasmon resonances (SPR), which undergo a shift towards longer wavelengths as the particle size increases[6,13].

In the spectrophotometer, the reference beam travels directly from the light source to the detector without interacting with the sample, while the sample beam exposes the sample to ultraviolet light with a continuously changing wavelength. When the wavelength matches the energy level required to promote an electron to a higher molecular orbital, energy is absorbed by the sample. The detector records the ratio of intensities between the reference and sample beams (Io/I). The computer identifies the wavelength at which the sample absorbed a significant amount of ultraviolet light by scanning for the largest difference between the two beams, plotting this wavelength as the peak ultraviolet light absorbance in the generated ultraviolet absorbance spectrum.

Before acquiring spectra, the ZnO nanoparticles (NPs) were re-dispersed 30 times in deionized water and subjected to ultrasonication. UV-visible spectroscopy analysis of ZnO NP reaction mixture was conducted at room temperature using a 10 mm pathlength quartz cuvette in a BioEra UV-Vis spectrometer, with a resolution of 1 nm over the wavelength range of 280-800 nm.

Characterization using FTIR :

FTIR characterization of synthesized NPs was done according to established protocols[9,11,13]. The analysis was performed on the FTIR model- Bruker Alpha II.

Characterization using X-ray diffraction (XRD):

The powder X-ray diffractometer technique was employed to determine the structure and composition of the synthesized ZnO nanoparticles. X-ray diffraction (XRD) relies on the constructive interference of monochromatic X-rays with crystalline samples.

X-rays are generated using a cathode ray tube, then filtered to produce monochromatic radiation, and collimated to concentrate before being directed towards the sample. When the incident rays interact with the sample, they create constructive interference according to Bragg's Law ($n\lambda=2d \sin\theta$), resulting in a diffracted ray. These diffracted X-rays are

then detected and counted, generating characteristic X-ray spectra. The specific wavelengths observed are unique to the target material[9,11]. The diffraction pattern of the synthesized nanoparticles was measured within the range of $2 < 2\theta < 70$ degrees.

X-ray diffraction (XRD) analysis of the prepared ZnO nanoparticles was conducted using a model XPERT-PRO X-ray diffractometer, operating at 45kV and a current of 40 mA, utilizing Cu K radiation in a θ-2θ configuration[13,22].

Characterization using Scanning Electron Microscopy (SEM) :

The Scanning Electron Microscope (SEM) was employed to achieve higher magnification and characterize the synthesized ZnO nanoparticles. SEM stands out as one of the most crucial and contemporary techniques for discerning NP morphologies. The nanoparticle powder was dispersed in deionized water via ultrasonication.

SEM generates an image by directing a highly focused electron beam, typically with energies ranging from 1 to 2 keV, across the sample and detecting the secondary electrons ejected. These secondary electrons originate from the surface of the sample and offer insights into its topography. The Scanning Electron Microscopy (SEM) analysis of the prepared metal nanoparticles was conducted using the JEOL Model JSM-6390LV [12].

Green synthesis of ZnO NPs :

The fabrication of ZnO NPs was done by green synthesis using *Citrus sinensis* fruit peels. The peel extract serves as both a reducing agent and a precursor for nanoparticle synthesis. These plant-synthesized ZnO NPs were confirmed using UV-visible spectroscopy. Furthermore, thorough characterization was performed using X-ray diffraction and scanning electron microscopy.

Characterization of ZnO NPs :

UV-Visible spectroscopy findings of ZnO NPs:

The absorption spectra of ZnO nanoparticles exhibit a surface plasmon resonance peak, depicted by an absorption maximum typically observed between 300-400 nm. As the size of the nanoparticles increases, the optical absorption spectra shift towards longer wavelengths. It was observed that the surface peaks varied depending on the size and concentration of metallic nanoparticles. The spectrum of ZnO nanoparticles is illustrated in Fig. 1. Given the broad distribution of shapes within the sample, it is evident that the characteristic absorption of these nanoparticles arises from the diverse contributions of various shapes and sizes, aligning with the observations made through electron microscopy. The sample showed highest absorption in between 300 to 400 nm indicating the material is oxide of zinc.

Characterization using FTIR :

A broad peak at 3402.22cm^{-1} in the 3600–3200 cm^{-1} range corresponds to strong O–H stretching, indicating the presence of hydroxyl groups, which may arise from adsorbed water or surface-bound organic functional groups. the other peak at 1637 cm^{-1} corelates to the presence of primary amines.

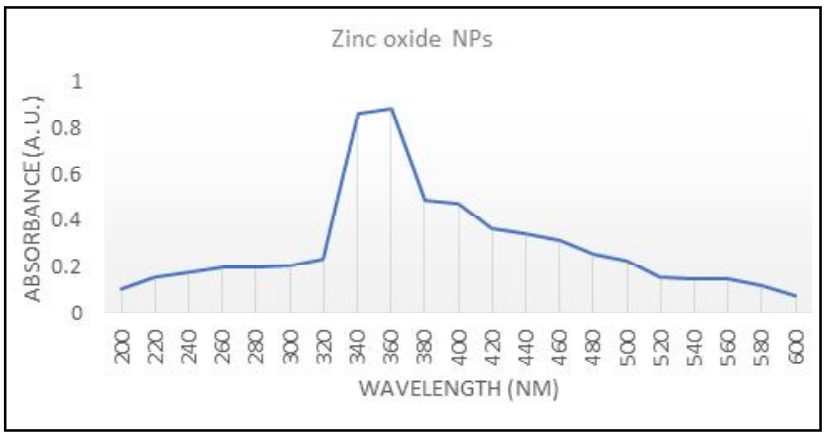

Fig. 1. UV-Visible absorption spectra of ZnO NPs

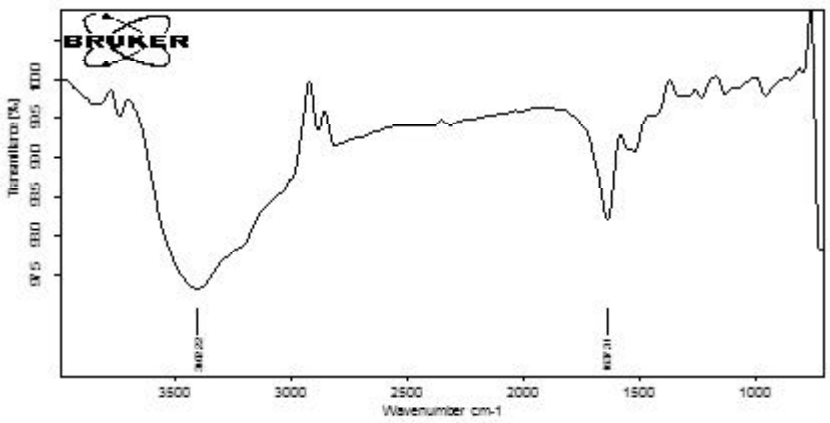

Fig. 2: FTIR spectra of ZnO NPs

The peak present in the range of 400-600 cm^{-1} is related to Zn-O stretching vibrations which suggest the synthesis of Zinc Oxide NPs [5].

X-ray diffraction (XRD) studies of ZnO NPs:

The XRD spectra indicate the crystalline nature of the ZnO nanoparticles. The Full Width at Half Maximum (FWHM) is a valuable metric for determining the size distribution of particles. A broader peak indicates a wider distribution of particle sizes. According to theoretical models, as particle size increases, so does the FWHM. The crystalline domain size was calculated from the width of the XRD peaks, assuming they are devoid of non-uniform strains, utilizing the Debye-Scherer formula.

By employing the Debye-Scherer equation to various peaks on the XRD graph of ZnO nanoparticles, it was observed that the particles exhibit diverse sizes. The average size of the ZnO nanoparticles was determined to be 48 nm. The X-ray diffraction pattern of sample is presented in the fig. 3.

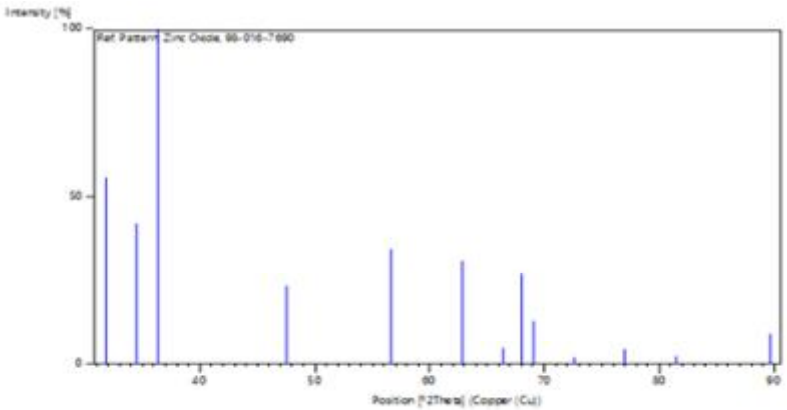

Fig. 3. X-ray diffraction pattern of ZnO NPs

Zeta-potential measurements and Particle size analysis of Zinc Oxide NPs :

Zeta-potential depicts the value of -20.7mV with a deviation of 6.74mV, it represents good stability and also that it is strongly anionic. the extract compounds get attached to the nanoparticles which results in negative surface charge and provide it more stability by inhibiting clumping of these nanoparticles together[8] (fig.4). The particle size distribution was measured at 25°C using water as the dispersion medium. The particle size of 80.94 nm is within the expected range for ZnO nanoparticles synthesized through green methods, confirming their successful production in required range.

Scanning Electron Microscopic (SEM) studies:

SEM analysis revealed that while the nanoparticles tended to agglomerate, a notable portion of them dispersed due to the energy imparted by the ultrasonic bath. Given the wide array of shapes present in the sample, it's evident that the distinctive absorption of these nanoparticles results from the diverse contributions of various shapes and sizes, which aligns with observations from the UV-Visible spectrum.

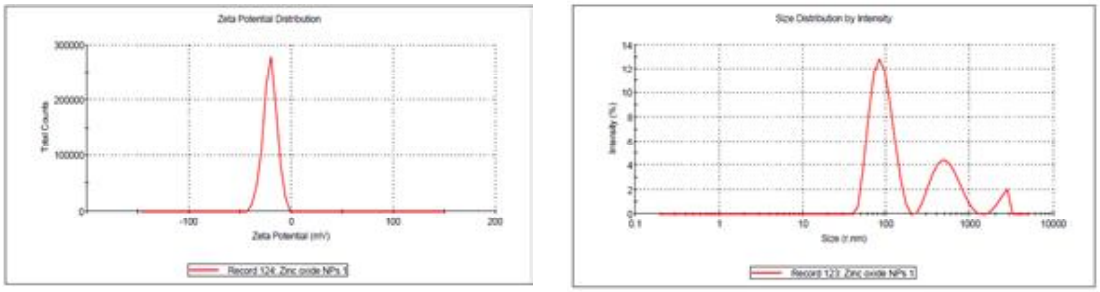

Fig. 4. Zeata potential measurement and particle size analysis of ZnO NPs.

High-resolution Scanning Electron Microscopy (SEM) provides insights into the surface morphology and structural characteristics of ZnO nanoparticles. These nanoparticles typically exist as individual crystallites, though they have a tendency to aggregate. The SEM image of ZnO nanoparticles illustrates that the majority exhibit a spherical shape, while a few are hexagonal or cubic in form, including multi-twinned nanoparticles with varying fold symmetries. The SEM image of the ZnO NPs sample is presented in Fig. 5.

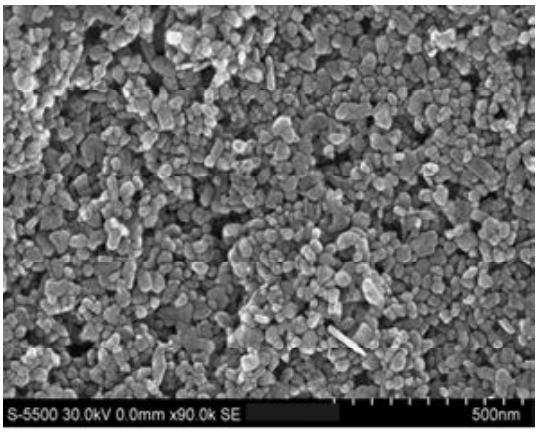

Fig. 5. SEM image of ZnO NPs sample

Maher *et al*.[13], synthesized ZnO NPs by green approach from *Sysimbrium irio* and characterized them using UV visible spectro-photometer, SEM, and TEM. A similar report was published by Kumar *et al.*,[12] demonstrating that the particle size of ZnO NPs was smaller than 70 nm and hexagonal or irregularly spherical. Mi *et al*.[14] synthesized ZnO NPs, characterized them, and further demonstrated that they have a profound positive impact on the growth and development of rice crops. The curcumin-synthesized ZnO NPs revealed a size of slightly more than 100 nm and were more or less spherical[19]. Turkoglu *et al*.,[23] reported the synthesis of ZnO NPs and their positive enhancing role in boosting growth and yield of *Chinopodium quinoa* by protecting crops from abiotic stresses. Our report is in analogy with the above reports indicating the synthesis of ZnO NPs from plant extract and their characterization.

Effect of ZnO NPs on Germination Growth and Biomass of Spinach :

The effect of zinc oxide nanoparticles (ZnO NPs) on seed germination, plant height, and biomass was evaluated across five concentrations (0–400 ppm). Germination percentage (Table-1) remained unaffected at 100 ppm and 200 ppm, with 100% and 90% germination respectively, but declined sharply to 70% at 400 ppm, suggesting that higher concentrations exert inhibitory effects on early seedling establishment.

Plant height data at maturity (Table-2) revealed a positive growth response at lower concentrations, with the highest mean height recorded at 200 ppm (34.66 cm), compared to 26 cm in the control. However, plant height decreased at 300 ppm and further at 400 ppm, indicating a threshold beyond which ZnO NPs negatively impact vegetative growth.

Biomass measurements (Table-3) followed a similar trend. Maximum biomass accumulation occurred at 200 ppm (26 g), reflecting enhanced physiological activity at moderate nanoparticle levels. Conversely, biomass significantly declined at 300 ppm and reached the lowest values at 400 ppm (13.16 g), demonstrating toxicity at elevated concentrations[8].

Table-1. Percent germination after treatment with different concentrations of ZnO NPs

Set No.	Conc. of Zinc Oxide NPs in ppm				
	Control	100 ppm	200 ppm	300 ppm	400 ppm
Seeds germinated	5	5	4	5	4
	5	5	5	4	3
Average	5	5	4.5	4.5	3.5
%germination	100	100	90	90	70

Table-2. Plant height (at the time of maturity) after treatment with different concentrations of ZnO NPs

Set No.	Conc. of Zinc Oxide NPs in ppm				
	Control	100 ppm	200 ppm	300 ppm	400 ppm
1	25	31	35	25	23
2	27	29	34	27	25
3	26	30	34	25	24
Average	26	30	34.66	26.33	24

Table-3. Biomass (gm) after treatment with different concentrations of ZnO NPs

Set No.	Conc. of Zinc oxide NPs in ppm				
	Control	100 ppm	200 ppm	300 ppm	400 ppm
1	15	21	26	18	13
2	17	21	27	21	13.5
3	16	21	25	19	13
Average	16	21	26	19.33	13.16

Overall, the results indicate that ZnO NPs exhibit concentration-dependent effects, with 100–200 ppm promoting growth, while concentrations above 300 ppm become inhibitory, reducing germination, height, and biomass[16-18].

The ZnO nanoparticles synthesized through the method outlined in this study offer numerous advantages compared to alternative green synthesis routes. This approach proves to be both energy and cost-efficient, yielding a high number of particles even with lower concentrations of plant extract.

Utilizing simple, laboratory-compatible green synthesis techniques employing plant waste, ZnO nanoparticles were synthesized

to yield nanocrystals with distinct structures and morphologies. The synthesized nanoparticles underwent characterization through UV-visible spectra, XRD, and SEM analyses. The powder X-ray diffractometer technique unveiled the structure and composition of the nanoparticles. High-resolution Scanning Electron Microscopy (SEM) revealed that the ZnO nanoparticles consist of nanocrystals with well-defined structures and morphologies. The average sizes of all the ZnO nanoparticles were determined to be within the range of 60-80 nm, which could be potentially used agriculture. The study demonstrates that ZnO NPs influence plant growth in a concentration-dependent manner. Moderate levels (100–200 ppm) enhance germination, plant height, and biomass, indicating a stimulatory effect, whereas higher concentrations (300–400 ppm) significantly reduce all parameters, showing clear phytotoxicity. Overall, ZnO NPs are beneficial only within an optimal range, beyond which they become inhibitory to plant development.

The authors are grateful to the Principal, Shri Shivaji College of Arts, Commerce and Science for providing the necessary equipment facility through CIC.

Conflicts of interest :

The authors declare that there is no conflict of interest related to the work presented in this paper.

Author contribution :

All experimental work was done by RK. RK & RG prepared a preliminary manuscript. RS reviewed and revised the manuscript and later submitted it to the Journal.

References :

1. Ahmed S, SA Chaudhry, and S. Ikram (2017). *J. Photochem. Photobiol.,* B *166*: 272–284.
2. Ajmal M, R Ullah, Z Muhammad, M Khan, HA. Kakar, AMK Kaplan, IA Okla, A Saleh, A Kamal, and Abdullah, (2023). *Molecules*, *28:* 5059.
3. Bala R, A Kalia, and S. Dhaliwal, (2019). *J. Soil Sci. Plant Nutri*, *19*: 379–389.
4. Batsmonova L, L Gonchar, NY Taran, and A. Okanenko, (2013). *Proceedings of the International Conference* Nanomaterials: Applications and Properties, pp. 2-5.
5. Bibi I, N Nazar, S Ata, M Sultan, A. Ali, and A Abbas (2019). *J. Mater. Res. Technol. 8* (6): 6115-6124.
6. Brause R, H Moeltgen and K. Kleinermanns (2002). *Applied Physics B: Lasers and Optics, 75*: 711-716.
7. El-Zohri M, NA Al-Wadaani, and SO Bafeel, (2021). *Plants*, *10*: 2400.
8. Fawziah, A., A. Mayasar, A. Nada, B. Fatima, A. Abeer, and M. Mohamed, (2023). *J. King Saud University-Science, 35*(1): 102434.
9. James R C. (2007). *Introduction to X-ray powder diffraction*. Springer. London, 2007.
10. Kaviya S, J Santhanalakshmi, B Viswanathan, J Muthumary, and K. Srinivasan (2011). *Acta A Mol. Biomol. Spectrosc. 79*: 594–598.
11. Kittel C. (1971). *Introduction to solid state physics*. John Wiley and Sons. New York, 1971.
12. Kumar R, S Mushtaq, and Sweta. (2023). *Authorea*, 168692943
13. Maher S, S Nisar, SM Aslam, F Saleem,

F Bahlil, M Imran, MA Assiri, A Nouroz, N Naheed, ZA Khan and P. Aslam (2023). *ACS Omega*, *8*(18): 15920-15931.

14. Mi K, X Yuan, Q Wang, C Dun, R Wang, S Yang, Y Yang, H Zhang and H Zhang, (2023). *Frontiers Plant Sci., 14*: 1196201.
15. Mie R, MW Samsudin, LB Din, A Ahmad, N Ibrahim, and SN. Adnan, (2014). *Inter. J. Nanomedicine, 9*: 121–127.
16. Raliya R, and J. Tarafdar (2013). *Agricultural Research*, *2*(1): 48–57.
17. Rico CM. (2011). *J. Agricul. Food Chem, 59*(8): 3485–3498.
18. Singh A, (2019). *Ecotoxicol. Environmental Safety*, *180*: 656–663.
19. Saif A, MO Omer, A S inattar, Y Tipu, HM Alharbi, U Saher, and T. Awan (2024), *ACS Omega*, 4c01489
20. Sidra S, A Muhammad, and K. Sunbal (2014). *The Scientific World* 1-8.
21. Srivastav A, D Ganjewala, RK Singhal, VD Rajput, T Minkina, M. Voloshina S Srivastava, and M. Shrivastava (2021). *Plants (Basel)*, *10*(12): 2556.
22. Swee-Yong P, L Wen-Pei, and A. Azizan (2012). *Inter J. Inorganic Chemi.,* 608183.
23. Türkoğlu A., K Haliloğlu, M Ekinci, M Turan, E Yildirim, Hİ. Öztürk, AAL Stansluos, H Nadaroğlu, M Piekutowska, and G. Niedbała (2024). *Agronomy*, *14* : 1462.
24. Zhang H, R Wang, Z Chen, P Cui, H Lu, Y Yang, and H. Zhang (2021) Agriculture, *11*: 1247.